



Published in final edited form as:

Cancer Cell. 2017 February 13; 31(2): 256–269. doi:10.1016/j.ccell.2016.12.010.

Ect2-dependent rRNA synthesis is required for *KRAS/TP53*-driven lung adenocarcinoma

Verline Justilien¹, Syed A. Ali¹, Lee Jamieson¹, Ning Yin¹, Adrienne D. Cox², Channing J. Der², Nicole R. Murray¹, and Alan P. Fields^{1,*}

¹Department of Cancer Biology, Mayo Clinic Comprehensive Cancer Center, Jacksonville, FL, USA

²Lineberger Comprehensive Cancer Center, University of North Carolina at Chapel Hill, Chapel Hill, NC, USA

SUMMARY

The guanine nucleotide exchange factor (GEF) Epithelial Cell Transforming sequence 2 (Ect2) has been implicated in cancer. However, it is not clear how Ect2 causes transformation, and whether Ect2 is necessary for tumorigenesis in vivo. Here, we demonstrate that nuclear Ect2 GEF activity is required for *Kras-Trp53* lung tumorigenesis in vivo, and that Ect2-mediated transformation requires Ect2-dependent ribosomal DNA (rDNA) transcription. Ect2 activates rRNA synthesis by binding the nucleolar transcription factor Upstream Binding Factor 1 (UBF1) on rDNA promoters, and recruiting Rac1 and its downstream effector nucleophosmin (NPM) to rDNA. Protein kinase C α (PKC α)-mediated Ect2 phosphorylation stimulates Ect2-dependent rDNA transcription. Thus, Ect2 regulates rRNA synthesis through a PKC α -Ect2-Rac1-NPM signaling axis that is required for lung tumorigenesis.

Graphical abstract

***Correspondence & lead contact:** Alan P. Fields, Ph.D., Department of Cancer Biology, Mayo Clinic Comprehensive Cancer Center, Griffin Cancer Research Building, Rm. 212, 4500 San Pablo Road, Jacksonville, Florida 32224, fields.alan@mayo.edu.

Publisher's Disclaimer: This is a PDF file of an unedited manuscript that has been accepted for publication. As a service to our customers we are providing this early version of the manuscript. The manuscript will undergo copyediting, typesetting, and review of the resulting proof before it is published in its final citable form. Please note that during the production process errors may be discovered which could affect the content, and all legal disclaimers that apply to the journal pertain.

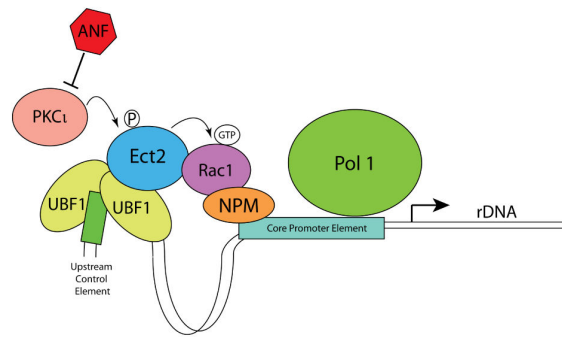
AUTHOR CONTRIBUTIONS

Conceptualization, V.J., S.A.A., N.R.M., and A.P.F.; Formal Analysis, V.J.; Investigation, V.J., S.A.A., L.J. and N.Y.; Resources, A.D.C., C.J.D. and A.P.F.; Writing – Original Draft Preparation, V.J. and A.P.F.; Review & Editing, V.J., A.D.C., C.J.D., N.R.M. and A.P.F.; Supervision, A.P.F.; Funding acquisition, V.J. and A.P.F.

The authors declare no conflicts of interest.

eTOC

Justilien et al. reveal that the guanine nucleotide exchange factor Ect2 is required for tumor initiation in a non-small cell lung carcinoma model and uncover a nuclear role for Ect2 in promoting rDNA transcription, which is important for transformation, through a mechanism involving Rac1, NPM, and UBF1.



Keywords

Ect2; Upstream Binding Factor 1 (UBF1); Nucleophosmin (NPM); Protein kinase; $\text{C}\alpha$ (PKC α); rRNA synthesis; tumor initiation

INTRODUCTION

Lung cancer is the leading cause of cancer deaths globally (Siegel et al., 2014). Lung adenocarcinoma (LADC), the most prevalent form of lung cancer, accounts for 40% of diagnoses (Ginsberg, 2001). Activating *KRAS* mutations are the most frequent oncogenic LADC driver, occurring in ~30% of cases (Salgia and Skarin, 1998). We recently identified Epithelial cell transforming sequence 2 (Ect2), a guanine nucleotide exchange factor (GEF) for Rho GTPases, as an oncogene in mutant *KRAS* LADC cells (Justilien and Fields, 2009; Justilien et al., 2011). Ect2 is overexpressed in LADC tumors and is required for transformed growth and invasion of LADC cells in vitro (Justilien and Fields, 2009; Justilien et al., 2011).

Ect2 regulates cytokinesis in non-transformed cells by activating RhoA (Kimura et al., 2000; Tatsumoto et al., 1999). During interphase, Ect2 is predominantly nuclear, where it is thought to be inactive, sequestered away from cytoplasmic RhoA (Tatsumoto et al., 1999). Mitotic nuclear envelope breakdown allows Ect2 to associate with the mitotic spindle (Hara et al., 2006). In lung cancer cells, a pool of Ect2 becomes mislocalized to the cytoplasm where it associates with the PKC α -Par6 complex and participates in transformed growth by activating Rac1, a process distinct from its role in cytokinesis (Justilien and Fields, 2009). More recently we demonstrated that nuclear Ect2 participates in transformed growth of ovarian cancer cells (Huff et al., 2013). However, neither the molecular mechanism(s) by which nuclear Ect2 participates in oncogenesis, nor a role for Ect2 in tumorigenesis in vivo has been elucidated. Here, we investigate the involvement of Ect2 in *Kras-Trp53*-mediated lung tumorigenesis.

RESULTS

Ect2 is required for *Kras-Trp53* mediated lung tumor formation

Ect2 is necessary for transformed growth of human LADC cells (Justilien and Fields, 2009; Justilien et al., 2011) but its role in LADC tumorigenesis in vivo is unknown. Therefore, we

crossed conditional *Ect2* knockout (*Ect2^{fl/fl}*) (Cook et al., 2011) and *LSL-Kras^{G12D};Trp53^{fl/fl}* (K,P) (Jackson et al., 2005) mice to generate tri-transgenic K,P,*Ect2^{fl/fl}* mice, and initiated lung tumorigenesis by intratracheal instillation of adenovirus expressing Cre-recombinase (Ad-Cre) as described previously (Regala et al., 2009). K,P mice exhibited a mean survival of 121 days whereas K,P,*Ect2^{fl/fl}* mice lived significantly longer (177 days) (Figure 1A). Histologic analysis revealed that K,P mice develop numerous LADC tumors, whereas K,P,*Ect2^{fl/fl}* mice exhibited fewer tumors (Figure 1B and C) and decreased tumor burden (Figure 1D). Tumor progression, assessed at survival endpoint, was not significantly different in K,P and K,P,*Ect2^{fl/fl}* tumors (Figure S1A) and no evidence for gender effects was observed (Figure S1B). A similar decrease in tumor number and burden was observed in K, *Ect2^{fl/fl}* mice compared to K mice indicating *Ect2* function is not dependent on *Trp53* loss (Figure S1C and D).

PCR of DNA from microdissected K,P,*Ect2^{fl/fl}* tumors revealed recombination of the *LSL-Kras^{G12D}* allele and both *Trp53^{fl/fl}* alleles, but incomplete recombination of the *Ect2^{fl/fl}* alleles (Figure 1E). QPCR of RNA from K,P and K,P,*Ect2^{fl/fl}* lung tumor cells revealed no significant difference in *Ect2* mRNA expression (Figure 1F), and immunohistochemistry confirmed that K,P and K,P,*Ect2^{fl/fl}* tumors express similar *Ect2* protein levels (Figure 1G). Thus, each K,P,*Ect2^{fl/fl}* tumor examined harbored an unrecombined *Ect2* allele and expressed abundant *Ect2*, indicating that *Kras/Trp53*-mediated lung tumorigenesis *in vivo* requires *Ect2*.

Ect2* drives transformed growth of *Kras/Trp53* lung tumor initiating cells *ex vivo

Tumors contain highly tumorigenic stem-like tumor-initiating cells (TICs) that drive tumor initiation, maintenance, relapse and metastasis (Chen et al., 2012; Driessens et al., 2012; Justilien et al., 2014; Schepers et al., 2012). The inability of K,P,*Ect2^{fl/fl}* mice to form tumors suggests that *Ect2* loss may impact the tumorigenicity of LADC TICs. CD24⁺/ITGB4⁺/NOTCH3^{hi} (3+) lung epithelial cells correspond to a TIC population in K,P LADC (Zheng et al., 2013). K,P 3+ cells comprise ~8% of the total K,P tumor cell population (Figure 2A) and exhibit enhanced growth as transformed oncospheres compared to the total K,P tumor cell population (Figures 2B and C). Lentiviral shRNA-mediated knockdown (KD) of *Ect2* using two mouse-specific *Ect2* shRNAs (Figure 2D) significantly inhibited oncosphere formation in K,P 3+ cells *ex vivo* (Figure 2E). Interestingly, 3+ cells are present in K,P,*Ect2^{fl/fl}* tumors (K,P,*Ect2^{fl/fl}* 3+ cells) at a similar frequency to K,P 3+ cells (Figure S2A), and exhibit oncosphere growth comparable to K,P 3+ cells (Figures S2B and S2C). This result was not unexpected since K,P,*Ect2^{fl/fl}* tumor cells retain an unrecombined *Ect2* allele and express abundant *Ect2* RNA and protein (see Figures 1E-G). However, Ad-Cre treatment of K,P,*Ect2^{fl/fl}* 3+ cells *ex vivo* led to efficient recombination of the remaining *Ect2* allele (Figure S2D), and a corresponding loss of *Ect2* mRNA (Figure 2F) and oncosphere formation (Figure 2G), similar to that observed after *Ect2* KD in K,P 3+ cells (Figure 2E). Thus, either *Ect2* KD or genetic *Ect2* ablation blocks tumorigenic growth of K,P 3+ cells *ex vivo*, reflecting the inability of K,P,*Ect2^{fl/fl}* mice to develop tumors *in vivo*.

Nuclear Ect2 GEF activity is required for LADC tumorigenesis

Ect2 localizes predominantly to the nucleus of non-transformed cells (Tatsumoto et al., 1999) presumably in an auto-inhibited state sequestered away from cytoplasmic Rho GTPases (Hara et al., 2006). However, we recently showed that nuclear Ect2 GEF activity is necessary for transformed growth of ovarian cancer cells (Huff et al., 2013). We therefore generated a GEF-deficient Ect2 mutant (DH^{mut} Ect2) (E428A and N608A within the Dbl homology (DH) domain); and NLS^{mut} Ect2 (five key arginine residues in the Ect2 NLS changed to alanines; R348,349,350,370,372A) (Rossman et al., 2005) (Figure 3A). Expression of HA-tagged wild-type (WT), DH^{mut} or NLS^{mut} Ect2 in A549 human LADC cells harboring oncogenic *KRAS* mutation revealed that WT and DH^{mut} Ect2 are predominantly nuclear, whereas NLS^{mut} Ect2 is largely cytoplasmic by immunofluorescence (Figure 3B) and cellular fractionation (Figure 3C). To assess function, we knocked down endogenous Ect2 using a previously characterized Ect2 shRNA, and expressed HA-tagged WT, DH^{mut} or NLS^{mut} Ect2 cDNAs made resistant to Ect2 KD to levels similar to endogenous Ect2 as described previously (Justilien et al., 2011) (Figure 3D). As expected (Justilien and Fields, 2009; Justilien et al., 2011) Ect2 KD inhibited soft agar growth that was restored by WT Ect2, but not by DH^{mut} or NLS^{mut} Ect2 (Figure 3E). Similar results were observed in two other human mutant *KRAS* LADC cell lines (H358 and H23) (Figures S3A-D), and in K,P 3+ cells (Figure 3F-H).

A hallmark of LADC TICs is their ability to initiate tumors in vivo. Consistent with their TIC phenotype, K,P 3+ cells generated tumors histologically similar to K,P tumors (Figure S3E). To assess the role of Ect2 in K,P 3+ cell tumor formation in vivo, we injected 3+ Ect2KD cells expressing empty vector, or WT, DH^{mut} or NLS^{mut} Ect2 into the flanks of non-transgenic syngeneic mice. Ect2 KD inhibited K,P 3+ cell-derived tumor formation (Figures 3I and 3J), and WT Ect2 reconstituted tumor growth whereas DH^{mut} and NLS^{mut} Ect2 did not (Figures 3I and 3J). Thus, K,P 3+ cells require nuclear Ect2 GEF activity for transformed growth ex vivo, and tumor formation in vivo.

Nuclear Ect2 is dispensable for cytokinesis

Previous work suggested that the roles of Ect2 in cytokinesis and transformation are distinct (Justilien and Fields, 2009). To directly test this hypothesis, we knocked down Ect2 and re-expressed either empty vector or shRNA-resistant WT, DH^{mut} or NLS^{mut} Ect2 in Madin-Darby canine kidney (MDCK) epithelial cells as previously described (Justilien and Fields, 2009) (Figure 4A). As expected (Justilien and Fields, 2009), Ect2 KD impaired cytokinesis, leading to an accumulation of multinucleated cells; whereas exogenous WT Ect2 rescued this cytokinesis defect, DH^{mut} Ect2 did not rescue, confirming that Ect2 GEF activity is required for cytokinesis (Figures 4B and 4C). Interestingly, NLS^{mut} Ect2, which does not support transformed growth of LADC cells (Figure 3), rescued cytokinesis in Ect2 KD MDCK cells. Thus, nuclear Ect2 is required for transformed growth but not cytokinesis.

We next assessed if the effect of Ect2 loss on K,P tumor formation is due to a cytokinesis defect. Lung epithelial cells from non-transgenic (NTg), Ect2^{fl/fl}, K,P or K,P,Ect2^{fl/fl} mice were infected with Ad-Cre to activate the *Kras*^{G12D} allele, and inactivate the *Trp53*^{fl/fl} and *Ect2*^{fl/fl} alleles as confirmed by PCR analysis (Figure 4D). Ad-Cre led to a significant

increase in Ect2 mRNA in K,P cells (Figure 4E), consistent with the elevated Ect2 observed in LADC cell lines and primary LADC tumors (Justilien and Fields, 2009). In contrast, Cre-induced genetic *Ect2* ablation resulted in loss of Ect2 mRNA in Ect2^{fl/fl} and K,P,Ect2^{fl/fl} cells (Figure 4E). Ect2 loss caused an accumulation of multi-nucleated cells in Ect2^{fl/fl} cells compared to NTg cells (Figure 4F), but not in K,P,Ect2^{fl/fl} cells compared to K,P cells (Figure 4F). Thus, Ect2 loss induces a cytokinesis defect in non-transformed mouse lung epithelial cells but not in transformed K,P cells consistent with previous publications suggesting that Ect2 transforming activity is uncoupled from cytokinesis (Justilien and Fields, 2009; Kanada et al., 2008).

Nuclear Ect2 associates with ribosomal processing proteins

We next immunoprecipitated nuclear Ect2 from A549 cells and identified associated proteins by mass spectrometry (Table S1). KEGG pathway analysis revealed enrichment in proteins involved in ribosome biogenesis (Table S2), and particularly in ribosomal DNA (rDNA) transcription and processing (Table S3). Interrogation of the Cancer Genome Atlas (TCGA) human LADC dataset (517 tumors) revealed significant co-expression of Ect2 with a majority (162/286) of genes critical to ribosome biogenesis (Tafforeau et al., 2013) (Figure 5A). This association was significantly stronger for Ect2 than other Rho GEFs (Figure 5A; see also Figure S4A), indicating a selective involvement of Ect2 in ribosome biogenesis. Similar results were obtained when only mutant *KRAS* LADC tumors were analyzed (Figure S4B). QPCR analysis of RNA from archived mutant *KRAS* LADC cases (n=19) revealed a significant positive correlation ($R^2=0.72$) between Ect2 mRNA and 45S pre-ribosomal RNA, a direct measure of rDNA transcription (Figure 5B). Kaplan-Meier analysis of the LADC TCGA dataset revealed that Ect2 expression is associated with decreased disease-free and overall survival (Figure S4C and D), indicating the clinical relevance of Ect2 signaling in LADC.

Confocal immunofluorescence microscopy revealed a significant pool of Ect2 co-localizing with Upstream Binding Factor 1 (UBF1), the major rDNA transcription factor, within the nucleolus in A549 cells (Figure 5C). Similar results were obtained in H358 and H23 cells (Figure S4E). Immunogold electron microscopy confirmed nucleolar Ect2 localization (Figure S4F), and reciprocal immunoprecipitations validated that endogenous UBF1 and Ect2 directly interact (Figure 5D). Similar results were observed in H23 and H358 cells (Figure S4G). Interestingly, Ect2 binding to UBF1 was not detected in nuclear extracts from non-transformed lung epithelial cells (Figure S4H) suggesting this interaction is preferentially present in LADC cells.

Ect2 regulates rRNA synthesis

UBF1 binds rDNA to regulate rDNA transcription (Drygin et al., 2010). ChIP on ChIP assays revealed Ect2-UBF1 complexes that were most abundant near the rDNA promoter and transcriptional start site (Figure 5E, primers 1, 6 and 7). Similar results were obtained in H358 and H23 cells (Figure S4I). ChIP analysis of NT and Ect2 KD cells expressing WT, DH^{mut} or NLS^{mut} Ect2 revealed preferential binding of WT Ect2, but not DH^{mut} or NLS^{mut} Ect2, to rDNA (Figure 5F). Similar results were observed in H358 cells (Figure S4J).

QPCR showed a decrease in 45S pre-rRNA in Ect2 KD cells that is restored by expression of WT but not DH^{mut} or NLS^{mut} Ect2 (Figure 5G). Similar results were obtained in H358 and H23 cells (Figure S4K), and in K,P 3+ cells (Figure S4L). Thus, nuclear Ect2 regulates rDNA transcription in human and mouse LADC cells.

Rac1 is a critical effector of nuclear Ect2

Ect2 is a GEF for Rac1, Cdc42 and RhoA (Tatsumoto et al., 1999). Cellular fractionation revealed that RhoA and Rac1 localized to both the cytoplasm and nucleus of A549 cells, whereas Cdc42 was exclusively cytoplasmic (Figure 6A), consistent with published results (Huff et al., 2013; Lanning et al., 2003). Similar results were observed in H358 and H23 cells (Figure S5A). Mass spectrometry detected Rac1, but not RhoA, in nuclear Ect2 immunoprecipitates (Table S1A). Thus we expressed a nucleotide-free Rac1 mutant that tightly binds GEFs (FLAG-G15A-Rac1), and immunoprecipitated it from nuclear extracts of A549 cells. Immunoblot analysis revealed that Ect2 directly binds nuclear Rac1 (Figure 6B). Pulldown assays revealed that Ect2 KD decreased active, GTP-bound nuclear Rac1 which is restored by expression of WT but not DH^{mut} nor NLS^{mut} Ect2 (Figure 6C, upper panel). This effect was Rac1-specific since nuclear RhoA activity was unaffected (Figure 6C, lower panel). Similar results were observed in H358 and H23 cells (Figures S5B and S5C). The inability of NLS^{mut} Ect2 to activate nuclear Rac1 was not due a lack of Ect2 GEF activity since this mutant, like WT Ect2, led to an increase in active cytoplasmic Rac1, whereas the DH^{mut} Ect2 did not (Figure S5D).

We next assessed whether Rac1, like Ect2, associates with UBF1 on rDNA repeats. ChIP on ChIP assays for UBF1 and Rac1 revealed Rac1 associated with UBF1 at the rDNA promoter and transcriptional start site (Figure 6D). Similar results were observed in H358 and H23 cells (Figures S5E). ChIP analysis revealed that Rac1 binding is inhibited by Ect2 KD and rescued by expression of WT Ect2, but not DH^{mut} or NLS^{mut} Ect2 (Figure 6E). Thus, Rac1 binds rDNA in an Ect2-, UBF1-dependent manner. Similar results were obtained in H358 cells (Figure S5F).

We next determined if Rac1 is required for rDNA transcription and transformed growth. Rac1 KD using two lentiviral shRNAs significantly decreased 45S rRNA (Figure 6F) and soft agar growth (Figure 6G). Furthermore, expression of a constitutively active Rac1 allele, caRac1, in Ect2 KD cells rescued 45S rRNA levels and soft agar growth (Figure 6H and I). Similar results were obtained in H358 and H23 cells (Figures S5G-I). Thus, Ect2 stimulates rDNA transcription by recruiting and activating Rac1 on rDNA.

Nucleophosmin (NPM) mediates nucleolar Ect2-Rac1 signaling

The nucleolar protein nucleophosmin (NPM; also known as B23) binds rDNA promoters and remodels ribosomal chromatin to activate rDNA transcription (Murano et al., 2008). NPM also binds Rac1 and may act as a chaperone for active nuclear Rac1 (Navarro-Lerida et al., 2015). Our proteomics identified NPM in nuclear Ect2 immunoprecipitates (Table S1A). Given the potential link between NPM and Rac1-dependent rRNA synthesis, we validated that NPM binds Rac1 in A549 cells using reciprocal immunoprecipitation (Figure 7A). Similar results were obtained in H358 and H23 cells (Figure S6A and B). NPM KD

inhibited 45S rRNA synthesis (Figure 7B) and soft agar growth (Figure 7C). Similar results were obtained in H358 and H23 cells (Figures S6C and D). ChIP analysis revealed that: 1) NPM binds rDNA, 2) both Rac1 and Ect2 KD inhibit NPM binding to rDNA, and 3) caRac1 rescues NPM binding to rDNA in Ect2 KD cells (Figure 7D). Similar results were obtained in H358 cells (Figures S6E). Thus, NPM is recruited to rDNA in an Ect2-, Rac1-dependent fashion and is a critical effector of Ect2-, Rac1-mediated rDNA transcription and transformed growth. Furthermore, UBF1 KD (Figure 7E, inset) inhibits Ect2, Rac1 and NPM binding to rDNA (Figure 7E). Similar results were obtained in H358 cells (Figure S6F).

PKC α -mediated phosphorylation regulates ECT2-dependent rRNA synthesis

PKC α phosphorylates Ect2 on Thr328 to regulate Ect2-dependent LADC transformation (Justilien et al., 2011). Thus, we expressed WT Ect2, and the phospho-Ect2 mutants T328A and T328D in Ect2 KD cells (Figure 8A). Cellular fractionation revealed that all three Ect2 alleles localize predominantly to the nucleus as expected (Figure 8B). Ect2 KD caused a decrease in 45S rRNA synthesis that could be rescued by WT Ect2 or T328D Ect2 but not T328A Ect2 (Figure 8C). Moreover, Ect2 KD led to a decrease in Ect2 (Figure 8D), Rac1 (Figure 8E) and NPM (Figure 8F) binding to rDNA that was efficiently rescued by WT Ect2 or T328D Ect2 but only weakly by T328A Ect2. Consistent with these results, WT and T328D Ect2 efficiently bound UBF1, whereas T328A Ect2 exhibited decreased UBF1 binding (Figure 8G). Functionally, WT and T328D Ect2 restored soft agar growth in Ect2 KD cells whereas T328A Ect2 did not (Figure 8H). Similar results were observed in H358 and H23 cells (Figure S7A and B). Thus, PKC α -mediated Ect2 phosphorylation stimulates 45S rDNA transcription by facilitating binding of Ect2 to UBF1, and subsequent recruitment of Rac1 and NPM to rDNA.

The anti-rheumatoid agent auranofin (ANF), a selective inhibitor of oncogenic PKC α signaling, inhibits LADC transformed growth ex vivo and tumor formation in vivo (Ali et al., 2016; Erdogan et al., 2006; Regala et al., 2008; Stallings-Mann et al., 2006). Consistent these data, ANF also exhibits dose-dependent inhibition of transformed growth of K,P tumor cells (Figure S7C). Furthermore, ANF treatment inhibited T328 phosphorylation of nuclear Ect2 (Figure S7D), binding of Ect2, Rac1 and NPM to rDNA (Figure 8I), and 45S RNA transcription (Figure 8J). As expected, Ect2 KD inhibited 45S rRNA, and ANF had no further inhibitory effect in Ect2 KD cells (Figure S7E). Interestingly, expression of WT Ect2 in Ect2 KD cells restored 45S rRNA and sensitivity to ANF-mediated 45S rRNA inhibition, whereas expression of T328D Ect2 or constitutive active Rac1 restored 45S rRNA and conferred resistance to the effects of ANF (Figure 8J). Thus, ANF inhibits 45S rRNA by inhibiting Ect2 phosphorylation and subsequent Ect2-, Rac1-dependent rDNA transcription. Consistent with the requisite role of enhanced rDNA transcription in transformed growth, the RNA polymerase I inhibitor CX-5461 exhibited dose-dependent inhibition of transformed growth of A549 cells (Figure S7F). CX-5461- and ANF-induced growth inhibition is associated with comparable ~50% decreases in 45S rRNA (Figure S7G), demonstrating that inhibition of 45S rRNA is sufficient to account for the growth inhibitory effects of CX-5461, ANF and genetic disruption of nuclear Ect2 signaling.

DISCUSSION

Ect2 is an oncogenic Rho GEF originally identified as a transforming gene in fibroblasts (Miki et al., 1993). The original transforming Ect2 clone lacked the N-terminal regulatory domain, and like other Dbl family GEFs, expression of this truncated Ect2 mutant resulted in aberrant, constitutive Ect2 GEF activity capable of cellular transformation (Saito et al., 2004). Full length Ect2 contains two nuclear localization signals (NLSs) that cause a predominantly nuclear localization in interphase cells (Tatsumoto et al., 1999). During mitosis, Ect2 distributes throughout the cytoplasm, and at cytokinesis localizes to the cleavage furrow where it activates RhoA-mediated scission (Tatsumoto et al., 1999). Early dogma was that nuclear Ect2 was auto-inhibited and physically sequestered from predominantly cytoplasmic GTPases (Hara et al., 2006). However, we recently reported that nuclear Ect2 GEF activity is required for transformed growth of ovarian cancer cells (Huff et al., 2013). Here, we validate and extend these observations, and establish that nuclear Ect2-mediated rDNA transcription is required for LADC transformation.

Previous studies suggested that the role of Ect2 in transformation is distinct from its role in cytokinesis (Justilien and Fields, 2009; Justilien et al., 2011). Ect2 KD does not induce a cytokinesis defect, despite inhibiting transformed growth of LADC, ovarian and fibrosarcoma cells (Justilien and Fields, 2009; Huff et al., 2013; Kanada et al., 2008). Our present data demonstrate that nuclear Ect2 is not necessary for cytokinesis in non-transformed cells, but is required for transformed growth of LADC cells. Furthermore, genetic deletion of Ect2 in non-transformed mouse lung epithelial cells results in accumulation of multi-nucleated cells indicative of a cytokinesis defect whereas Ect2 deletion in *Kras/Trp53*-transformed mouse lung epithelial cells inhibits transformed growth *ex vivo* without inducing a cytokinesis defect. Thus, the roles of Ect2 in cellular transformation and cytokinesis are distinct and separable. Whereas Ect2 activates RhoA during cytokinesis, nuclear Ect2 activates Rac1 in LADC cells to activate rDNA transcription. These results argue that *Kras-Trp53*-transformed lung epithelial cells have lost their requirement for Ect2-dependent cytokinesis, consistent with similar observations in human LADC cells (Justilien and Fields, 2009; Justilien et al., 2011), ovarian (Huff et al., 2013) and fibrosarcoma (Kanada et al., 2008) cells.

Our proteomics analysis indicated a role for Ect2 in ribosome biogenesis, a notion validated through biochemical and genetic analysis. Increased ribosome biogenesis is a common feature of transformed cells, which required elevated ribosome biosynthesis to support growth (Montanaro et al., 2008). Ribosome biogenesis involves the synthesis, processing and assembly of rRNA into ribosomal subunits. Cancer cells exhibiting elevated rDNA transcription are sensitive to the growth inhibitory effects of the Polymerase I inhibitor CX-5461 (Bywater et al., 2012), a finding confirmed here in K,P tumor cells. Regulation of rDNA transcription has been linked to the oncogenic drivers c-MYC, PI3K and RAS (Tsai and Pederson, 2014); for instance, c-MYC transformation requires c-Myc binding to the Pol I transcription machinery and elevated rDNA transcription (Grandori et al., 2005). Interestingly, rDNA transcription is negatively regulated by p53 (Tsai and Pederson, 2014), further linking increased rDNA transcription and malignant transformation. Though increased ribosome synthesis plays a direct causative role in cellular transformation, the

mechanistic link(s) between rDNA transcription and cancer are not well understood. Our data demonstrate that oncogenic nuclear Ect2 regulates rDNA transcription in LADC cells, and that Ect2-dependent rDNA transcription is required for LADC transformation. Ect2 binds UBF1, the major rDNA transcription factor, at the rDNA promoter, and Ect2 KD inhibits rDNA transcription. GEF-deficient Ect2 exhibits decreased UBF1 binding and is unable to reconstitute rDNA transcription in Ect2 KD cells underscoring the importance of Ect2 GEF activity in rDNA transcription. We find that Rac1 is the critical effector of Ect2 in rDNA transcription. Like Ect2, Rac1 associates with UBF1 on rDNA promoters, and Rac1 KD decreases rDNA transcription. Although nuclear Rac1 has been implicated in DNA damage response and RNA polymerase II-mediated transcription (reviewed in (Fritz and Henninger, 2015), our data demonstrate an additional role for Rac1 in rDNA transcription. Ect2-activated Rac1 recruits NPM to rDNA and stimulates rDNA transcription. Our data are consistent with a model in which Ect2 binds UBF1 on rDNA promoters and recruits and activates Rac1 to drive rRNA synthesis by regulating the interaction of active Rac1 with NPM. Interestingly, PKC α -mediated Ect2 phosphorylation, which is required for oncogenic Ect2 function, regulates binding of Ect2 to UBF1, subsequent binding of Rac1 and NPM to rDNA, and rDNA transcription. Furthermore, the PKC α inhibitor ANF blocks Ect2 phosphorylation and Ect2-, Rac1-dependent rDNA transcription. These data provide a clinical rationale for the use of ANF to target the Ect2-Rac1-NPM signaling axis for treatment of *KRAS*-driven LADC.

Ect2 is overexpressed in many tumor types (Chen et al., 2015; Hirata et al., 2009; Huff et al., 2013; Jin et al., 2014; Justilien and Fields, 2009; Salhia et al., 2008; Sano et al., 2006; Zhang et al., 2008) and is required for transformed growth of many cancer cell types in vitro (reviewed in (Fields and Justilien, 2010). However, the importance of Ect2 in tumor formation in vivo was unknown. We establish that Ect2 is required for LADC tumor initiation and maintenance of a LADC TIC phenotype. Ect2 loss in *Kras*^{G12D}/*Trp53* mice leads to a profound loss of lung tumor formation that can be traced to a defect in TIC function. Ect2 loss also decreases rDNA transcription in *Kras*^{G12D}/*Trp53*-transformed lung TICs, indicating that Ect2-dependent rDNA transcription is intimately linked to the tumorigenic potential of Ect2. Our data provide mechanistic insight into Ect2-dependent transformation, enhance our understanding of the initiating events in *Kras*-mediated lung tumorigenesis, and establish PKC α -Ect2-Rac1-NPM signaling as a viable therapeutic target.

EXPERIMENTAL PROCEDURES

Antibodies and cell lines

Antibodies: Ect2 (Millipore, Billerica MA, USA), RhoA, NPM1 and UBF1 (Santa Cruz Biotechnology, Santa Cruz, CA, USA); Rac1 and Cdc42 (BD Transduction Labs, San Jose, CA, USA); HA, β -actin, MEK1 and Lamin A/C (Cell Signaling, Danvers, MA, USA); FLAG (Sigma-Aldrich, St Louis, MO, USA); Phalloidin-Alexa Fluor 594 (Invitrogen, Life Technologies Carlsbad, CA, USA). CD24-PerCp-eFluor[®]710 (eBioscience, San Diego, CA USA), Notch3-Alexa-Fluor[®]647 (Biolegend, San Diego, CA USA), and ITGB4-PE (Abcam, Cambridge, MA 02139-1517, USA). S-peptide monoclonal antibody and expression plasmid were a gift from Dr. S. Kaufmann, Mayo Clinic. The pT328-Ect2

antibody was described previously (Justilien et al., 2011). A549, H358, H23, BEAS-2B and MDCK cells were from the American Type Culture Collection (Manassas, VA, USA).

Generation of *LSL-Kras^{G12D};Trp53^{fl/fl};Ect2^{fl/fl}* mice and Ad-Cre intratracheal instillations

LSL-Kras^{G12D} and *Trp53^{fl/fl}* mice were mated to generate *LSL-Kras^{G12D};Trp53^{fl/fl}* (K,P) mice. K,P mice were mated to floxed *Ect2* mice (*Ect2^{fl/fl}*) (Cook et al., 2011) to generate K,P,*Ect2^{fl/fl}* mice. Non-transgenic (NTg), *Ect2^{fl/fl}* and *Trp53^{fl/fl};Ect2^{fl/fl}* littermates served as controls. Mice (6–10 weeks old) were anesthetized with ketamine/xylazine, intubated intratracheally and instilled with two 50- μ L aliquots of adenovirus-Cre recombinase (1.5×10^8 PFU/mL) (Vector Laboratories, Burlingame, CA, USA) as described previously (Fasbender et al., 1998). All animal experiments were approved by the Institutional Animal Care and Use Committee of Mayo Clinic.

Survival study

Animals were inspected daily for health and moribund animals were euthanized by CO₂ asphyxiation for necropsy. Criteria for euthanasia were based on independent veterinary assessment using AAALAC guidelines; animals in a condition considered incompatible with continued survival were considered deaths. Animals removed at sacrifice or found dead with confirmed lung tumors were considered as censored deaths.

Histology and immunohistochemistry

Mice were sacrificed, exsanguinated, and lungs processed for histologic and immunohistochemical analysis as previously described (Regala et al., 2009). Mouse *Ect2* was visualized using an *Ect2* antibody and the Envision Plus Dual Labeled Polymer Kit following the instructions of the manufacturer (DAKO, Carpinteria, CA, USA). Slide images were captured and analyzed using a ScanScope scanner and ImageScope software (Aperio Technologies, Buffalo Grove, IL).

LSL-Kras^{G12D}, Trp53^{fl/fl}, and Ect2^{fl/fl} allele status

Allele status was determined by PCR as described (Regala et al., 2009; Zheng et al., 2013) using the primers listed in **Supplemental Experimental Procedures**.

Primary lung epithelial cell isolation

Tumor tissue was dissected from Ad-Cre-instilled K,P or K,P,*Ect2^{fl/fl}* mice or total lung from Nt, *Ect2^{fl/fl}* K,P and K,P,*Ect2^{fl/fl}* mice and processed for lung epithelial cell isolation as previously described (Regala et al., 2009).

FACS analysis

CD24+/*ITGB4*+/*NOTCH3*^{hi} (3+) cells were isolated from from K,P or K,P,*Ect2^{fl/fl}* lung tumor cells by staining with CD24-PerCp-eFluor®710 (eBioscience, San Diego, CA), Notch3-Alexa-Fluor®647 (Biolegend, San Diego, CA), and *ITGB4*-PE (Abcam, Cambridge, MA) in 10% Fetal Bovine Serum in 1x phosphate-buffered saline (PBS) at 4°C for 30 min in the dark with gentle agitation. SYTOX Green (ThermoFisher Scientific, Grand Island, NY)

was used to discriminate live and dead cells. Labeled cells were subjected to fluorescent activated cell sorting on a FACS Aria (BD San Jose, CA) as described (Zheng et al., 2013).

Ex vivo culture

CD24⁺/ITGB4⁺/NOTCH3^{hi} cells were resuspended in BEGM without hydrocortisone (Lonza, Walkersville, MD) containing 10 ng/mL of keratinocyte growth factor (PeproTech, Rocky Hill, NJ, USA), 5% charcoal stripped fetal bovine serum and 50% Matrigel (BD Biosciences, San Jose, CA, USA), and plated on Matrigel-coated tissue culture wells topped with BEGM. Medium was changed twice weekly. Self-renewal was assessed in oncospheres released from Matrigel using Cell Recovery Solution (BD Biosciences). Cells were disassociated into single cells by triturating with StemPro® Accutase (Invitrogen, life technology) and assessed for oncosphere size and number 2 weeks after being plated in 96-well Matrigel-coated plates. In some experiments, total lung epithelial cells isolated from NTg, Ect2^{fl/fl}, K,P and K,P,Ect2^{fl/fl} mice were plated as described above and infected with Ad-Cre (MOI 50). Cells were released from Matrigel culture using BD Cell Recovery Solution (BD Biosciences) and total RNA and DNA were isolated for analysis.

Lentiviral RNAi, cell transduction, plasmids, transfections, and immunoblot analysis

Lentiviral vectors containing human and mouse Ect2, Rac1, NPM1, UBF1 or a non-target control (NT) shRNA were obtained from Sigma, packaged into recombinant lentivirus, and used to establish stable cell transfectants as described previously (Frederick et al., 2008). The human HA-tagged RNAi-resistant ECT2 lentivirus was described previously (Justilien and Fields, 2009). The Ect2 GEF-deficient and NLS mutants were generated as previously described (Huff et al., 2013). The T328A and T328D Ect2 phospho-mutants were described previously (Justilien et al., 2011). Ect2 cDNAs were packaged into lentiviral vectors as previously described (Frederick et al., 2008), and cells stably transduced with lentiviral Ect2 alleles were produced as described previously (Huff et al., 2013). Nucleotide free Flag-Rac1G15A and Myc-caRac1V12 (caRac1) plasmids were gifts of Dr. P.Z. Anastasiadis (Mayo Clinic). Efficiency of Ect2, Rac1, UBF1 and NPM1 knockdown and expression of Ect2 and Rac1 cDNAs was assessed by QPCR and immunoblot analysis as previously described (Regala et al., 2005).

Subcellular fractionation and immunoprecipitation

Cells were fractionated using NE-PER (Pierce Biotechnology, Rockford, IL, USA) as previously described (Justilien and Fields, 2009). Nuclear and cytoplasmic fractions were assessed for purity by Lamin A/C and MEK1 immunoblot analysis.

Multinucleated cell analysis

Cells grown on glass chamber slides (Nalge Nunc International, Naperville, IL, USA) were fixed, permeabilized and stained with phalloidin Alexa Fluor 594 and 4',6 diamidino-2-phenylindole (DAPI) (Vectashield; Vector Laboratories, Burlingame, CA, USA) as previously described (Justilien and Fields, 2009). Representative fields were photographed at 20x magnification, and >1000 cells from each cell type were analyzed for multiple nuclei.

Mass spectrometry and pathway analysis

Cells expressing empty FLAG-vector or FLAG-WT-Ect2 were fractionated and nuclear fractions subjected to FLAG immunoprecipitation as described above. Mass spectrometry was performed as previously described (Justilien et al., 2011; Justilien et al., 2014). KEGG pathway analysis was performed on Ect2-associated proteins represented in our proteomics analysis by >2 unique peptides using the David Bioinformatics Resource.

Chromatin immunoprecipitation (ChIP)

ChIP was performed to assess occupancy of NPM1, or co-occupancy of UBF with Ect2 or Rac1, on rDNA as follows: Cells were crosslinked with 1% formaldehyde, lysed and cytoplasmic protein fractions discarded. Nuclear fractions were sonicated to obtain DNA fragments of ~500 bp as determined by agarose gel electrophoresis and ethidium bromide staining. Pre-cleared supernatants were first incubated with a NPM1, UBF or IgG control antibody (Santa Cruz Biotechnology) overnight followed by 3 hr (4°C) incubation with Protein A/G-conjugated agarose beads (Santa Cruz Biotechnology). Protein A/G bead complexes were washed and protein-DNA complexes were eluted in 1% SDS and 100 mM NaHCO₃. For co-occupancy experiments, eluants were subjected to a second ChIP with Ect2 or Rac1 antibody. Crosslinks were reversed by incubation overnight in elution buffer containing 200 mM sodium chloride. DNA was extracted, purified, precipitated and resuspended in Tris-EDTA for QPCR using primer sets spanning the human rDNA repeat (primers listed in **Supplemental Experimental Procedures**). QPCR was performed using SYBR® Green (Life Technologies, Grand Island, NY) dye detection on an Applied Biosystems ViiA7 thermal cycler and results quantified by the comparative Ct method.

RNA isolation and 45S rRNA expression

Total RNA was isolated from cells using the RNeasy Plus Mini Kit (Qiagen, Valencia, CA) and from primary LADC tumors using RNAqueous (Ambion, Austin, TX, USA). 45S pre-rRNA abundance was assessed by QPCR using SYBR-green as described above. 45S pre-rRNA levels were normalized to β-actin.

Rac1 and RhoA activity assays

Nuclear Rho GTPase activity was determined in nuclear lysates by affinity pulldown as previously described (Justilien and Fields, 2009).

Transformation and tumorigenicity assays

Human LADC cell lines and KP tumor cells were assessed for transformed growth in soft agar as previously described (Regala et al., 2005). In some experiments, ANF (Santa Cruz Biotechnology, Santa Cruz, CA, USA), the RNA polymerase I inhibitor CX-5461 (EMD Millipore, Billerica, MA), or diluent was added to the cultures at the concentrations indicated in the figure legend. 1×10^5 CD24+/ITGB4+/NOTCH3^{hi} cells were implanted subcutaneously in non-transgenic C57BL/6 syngeneic mice as previously described (Regala et al., 2005). Tumor volume and final tumor weight were assessed as previously described (Regala et al., 2005).

Analysis of TCGA Lung Adenocarcinoma Data

A TCGA lung adenocarcinoma dataset (517 cases) was interrogated for correlations between expression of *Ect2*, and of 17 Rho GEFs (listed in Figure 5A), and expression of 286 ribosomal processing genes (Tafforeau et al., 2013) using the mutual exclusivity/co-occurrence tool at cBioPortal for Cancer Genomics. P values were derived using the Fisher Exact T test. The TCGA LADC dataset was also interrogated for an association of *Ect2* mRNA with disease-free and overall survival using the survival analysis tool at cBioPortal and the LogRank Test to assess statistical significance.

Statistical Methods

Statistical analysis of animal survival was carried out using the Log-rank and Wilcoxon tests. Final tumor weights of KP 3+ TIC xenograft tumors were compared using one-way ANOVA. All other statistical analyses used a two-tailed Student's t-test to assess significance. P values of <0.05 were considered significant.

Supplementary Material

Refer to Web version on PubMed Central for supplementary material.

ACKNOWLEDGEMENTS

We thank Ben Madden (Mayo Clinic Proteomics Research Center) for mass spectrometric analysis; Capella Weems, Marie Chrest, Kayla Lewis, Hannah Orsech, Chynna Hendricks and Kathryn Brennan for technical assistance; Brandy Edenfield for immunohistochemistry; Dr. Laura Lewis-Tuffin for flow cytometry; Dr. Andras Khoo for pathology; and Dr. E. Aubrey Thompson and the Fields lab for critical feedback. This work supported by grants from National Institutes of Health/National Cancer Institute (R01 CA081436, R01 CA 180997, and R21 CA151250-02 to APF, R01 CA042978 to CJD/ADC; and R21 CA204938 to VJ), a Research Supplement to Promote Diversity in Health-related Research Award from the National Cancer Institute (VJ), and a George Haub Family Career Development Award in Cancer Research Grant (VJ). APF is the Monica Flynn Jacoby Professor of Cancer Research, an endowment fund providing partial support for the investigator's research program.

REFERENCES

- Ali SA, Justilien V, Jamieson L, Murray NR, Fields AP. Protein Kinase Ciota Drives a NOTCH3-dependent Stem-like Phenotype in Mutant KRAS Lung Adenocarcinoma. *Cancer Cell*. 2016; 29:367–378. [PubMed: 26977885]
- Bywater MJ, Poortinga G, Sanij E, Hein N, Peck A, Cullinane C, Wall M, Cluse L, Drygin D, Andres K, et al. Inhibition of RNA polymerase I as a therapeutic strategy to promote cancer-specific activation of p53. *Cancer Cell*. 2012; 22:51–65. [PubMed: 22789538]
- Chen J, Li Y, Yu TS, McKay RM, Burns DK, Kernie SG, Parada LF. A restricted cell population propagates glioblastoma growth after chemotherapy. *Nature*. 2012; 488:522–526. [PubMed: 22854781]
- Chen J, Xia H, Zhang X, Karthik S, Pratap SV, Ooi LL, Hong W, Hui KM. ECT2 regulates the Rho/ERK signalling axis to promote early recurrence in human hepatocellular carcinoma. *Journal of hepatology*. 2015; 62:1287–1295. [PubMed: 25617497]
- Cook DR, Solski PA, Bultman SJ, Kauselmann G, Schoor M, Kuehn R, Friedman LS, Cowley DO, Van Dyke T, Yeh JJ, et al. The *ect2* rho Guanine nucleotide exchange factor is essential for early mouse development and normal cell cytokinesis and migration. *Genes Cancer*. 2011; 2:932–942. [PubMed: 22701760]
- Driessens G, Beck B, Caauwe A, Simons BD, Blanpain C. Defining the mode of tumour growth by clonal analysis. *Nature*. 2012; 488:527–530. [PubMed: 22854777]

- Drygin D, Rice WG, Grummt I. The RNA polymerase I transcription machinery: an emerging target for the treatment of cancer. *Annu Rev Pharmacol Toxicol.* 2010; 50:131–156. [PubMed: 20055700]
- Erdogan E, Lamark T, Stallings-Mann M, Lee J, Pellicchia M, Thompson EA, Johansen T, Fields AP. Aurothiomalate inhibits transformed growth by targeting the PB1 domain of protein kinase Ciota. *J Biol Chem.* 2006; 281:28450–28459. [PubMed: 16861740]
- Fasbender A, Lee JH, Walters RW, Moninger TO, Zabner J, Welsh MJ. Incorporation of adenovirus in calcium phosphate precipitates enhances gene transfer to airway epithelia in vitro and in vivo. *J Clin Invest.* 1998; 102:184–193. [PubMed: 9649572]
- Fields AP, Justilien V. The guanine nucleotide exchange factor (GEF) Ect2 is an oncogene in human cancer. *Adv Enzyme Regul.* 2010; 50:190–200. [PubMed: 19896966]
- Frederick LA, Matthews JA, Jamieson L, Justilien V, Thompson EA, Radisky DC, Fields AP. Matrix metalloproteinase-10 is a critical effector of protein kinase Ciota-Par6alpha-mediated lung cancer. *Oncogene.* 2008; 27:4841–4853. [PubMed: 18427549]
- Fritz G, Henninger C. Rho GTPases: Novel Players in the Regulation of the DNA Damage Response? *Biomolecules.* 2015; 5:2417–2434. [PubMed: 26437439]
- Ginsberg, R., Vokes, E., Rosenzweig, K. Non-small cell lung cancer. In: De Vitta, SHV., Rosenberg, S., editors. *Cancer: Principles and Practice of Oncology.* Lippencott Williams and Wilkins; Philadelphia, PA: 2001. p. 925-983.
- Grandori C, Gomez-Roman N, Felton-Edkins ZA, Ngouenet C, Galloway DA, Eisenman RN, White RJ. c-Myc binds to human ribosomal DNA and stimulates transcription of rRNA genes by RNA polymerase I. *Nature cell biology.* 2005; 7:311–318. [PubMed: 15723054]
- Hara T, Abe M, Inoue H, Yu LR, Veenstra TD, Kang YH, Lee KS, Miki T. Cytokinesis regulator ECT2 changes its conformation through phosphorylation at Thr-341 in G2/M phase. *Oncogene.* 2006; 25:566–578. [PubMed: 16170345]
- Hirata D, Yamabuki T, Miki D, Ito T, Tsuchiya E, Fujita M, Hosokawa M, Chayama K, Nakamura Y, Daigo Y. Involvement of Epithelial Cell Transforming Sequence-2 Oncoantigen in Lung and Esophageal Cancer Progression. *Clin Cancer Res.* 2009; 15:256–266. [PubMed: 19118053]
- Huff LP, Decristo MJ, Trembath D, Kuan PF, Yim M, Liu J, Cook DR, Miller CR, Der CJ, Cox AD. The Role of Ect2 Nuclear RhoGEF Activity in Ovarian Cancer Cell Transformation. *Genes Cancer.* 2013; 4:460–475. [PubMed: 24386507]
- Jackson EL, Olive KP, Tuveson DA, Bronson R, Crowley D, Brown M, Jacks T. The differential effects of mutant p53 alleles on advanced murine lung cancer. *Cancer Res.* 2005; 65:10280–10288. [PubMed: 16288016]
- Jin Y, Yu Y, Shao Q, Ma Y, Zhang R, Yao H, Xu Y. Up-regulation of ECT2 is associated with poor prognosis in gastric cancer patients. *International journal of clinical and experimental pathology.* 2014; 7:8724–8731. [PubMed: 25674238]
- Justilien V, Fields AP. Ect2 links the PKCiota-Par6alpha complex to Rac1 activation and cellular transformation. *Oncogene.* 2009; 28:3597–3607. [PubMed: 19617897]
- Justilien V, Jameison L, Der CJ, Rossman KL, Fields AP. Oncogenic activity of Ect2 is regulated through protein kinase C iota-mediated phosphorylation. *J Biol Chem.* 2011; 286:8149–8157. [PubMed: 21189248]
- Justilien V, Walsh MP, Ali SA, Thompson EA, Murray NR, Fields AP. The PRKCI and SOX2 oncogenes are coamplified and cooperate to activate Hedgehog signaling in lung squamous cell carcinoma. *Cancer Cell.* 2014; 25:139–151. [PubMed: 24525231]
- Kanada M, Nagasaki A, Uyeda TQ. Novel functions of Ect2 in polar lamellipodia formation and polarity maintenance during "contractile ring-independent" cytokinesis in adherent cells. *Mol Biol Cell.* 2008; 19:8–16. [PubMed: 17942602]
- Kimura K, Tsuji T, Takada Y, Miki T, Narumiya S. Accumulation of GTP-bound RhoA during cytokinesis and a critical role of ECT2 in this accumulation. *J Biol Chem.* 2000; 275:17233–17236. [PubMed: 10837491]
- Lanning CC, Ruiz-Velasco R, Williams CL. Novel mechanism of the co-regulation of nuclear transport of SmgGDS and Rac1. *J Biol Chem.* 2003; 278:12495–12506. [PubMed: 12551911]
- Miki T, Smith CL, Long JE, Eva A, Fleming TP. Oncogene ect2 is related to regulators of small GTP-binding proteins. *Nature.* 1993; 362:462–465. [PubMed: 8464478]

- Montanaro L, Trere D, Derenzini M. Nucleolus, ribosomes, and cancer. *The American journal of pathology*. 2008; 173:301–310. [PubMed: 18583314]
- Murano K, Okuwaki M, Hisaoka M, Nagata K. Transcription regulation of the rRNA gene by a multifunctional nucleolar protein, B23/nucleophosmin, through its histone chaperone activity. *Mol Cell Biol*. 2008; 28:3114–3126. [PubMed: 18332108]
- Navarro-Lerida I, Pellinen T, Sanchez SA, Guadamillas MC, Wang Y, Mirtti T, Calvo E, Del Pozo MA. Rac1 nucleocytoplasmic shuttling drives nuclear shape changes and tumor invasion. *Dev Cell*. 2015; 32:318–334. [PubMed: 25640224]
- Regala RP, Davis RK, Kunz A, Khor A, Leitges M, Fields AP. Atypical protein kinase C{iota} is required for bronchioalveolar stem cell expansion and lung tumorigenesis. *Cancer Res*. 2009; 69:7603–7611. [PubMed: 19738040]
- Regala RP, Thompson EA, Fields AP. Atypical protein kinase C iota expression and aurothiomalate sensitivity in human lung cancer cells. *Cancer Res*. 2008; 68:5888–5895. [PubMed: 18632643]
- Regala RP, Weems C, Jamieson L, Copland JA, Thompson EA, Fields AP. Atypical protein kinase Ciota plays a critical role in human lung cancer cell growth and tumorigenicity. *J Biol Chem*. 2005; 280:31109–31115. [PubMed: 15994303]
- Rossman KL, Der CJ, Sondek J. GEF means go: turning on RHO GTPases with guanine nucleotide-exchange factors. *Nat Rev Mol Cell Biol*. 2005; 6:167–180. [PubMed: 15688002]
- Saito S, Liu XF, Kamijo K, Raziuddin R, Tatsumoto T, Okamoto I, Chen X, Lee CC, Lorenzi MV, Ohara N, Miki T. Deregulation and mislocalization of the cytokinesis regulator ECT2 activate the Rho signaling pathways leading to malignant transformation. *J Biol Chem*. 2004; 279:7169–7179. [PubMed: 14645260]
- Salgia R, Skarin AT. Molecular abnormalities in lung cancer. *J Clin Oncol*. 1998; 16:1207–1217. [PubMed: 9508209]
- Salhia B, Tran NL, Chan A, Wolf A, Nakada M, Rutka F, Ennis M, McDonough WS, Berens ME, Symons M, Rutka JT. The guanine nucleotide exchange factors trio, Ect2, and Vav3 mediate the invasive behavior of glioblastoma. *Am J Pathol*. 2008; 173:1828–1838. [PubMed: 19008376]
- Sano M, Genkai N, Yajima N, Tsuchiya N, Homma J, Tanaka R, Miki T, Yamanaka R. Expression level of ECT2 proto-oncogene correlates with prognosis in glioma patients. *Oncol Rep*. 2006; 16:1093–1098. [PubMed: 17016598]
- Schepers AG, Snippert HJ, Stange DE, van den Born M, van Es JH, van de Wetering M, Clevers H. Lineage tracing reveals Lgr5+ stem cell activity in mouse intestinal adenomas. *Science*. 2012; 337:730–735. [PubMed: 22855427]
- Siegel R, Ma J, Zou Z, Jemal A. Cancer statistics, 2014. *CA Cancer J Clin*. 2014; 64:9–29. [PubMed: 24399786]
- Stallings-Mann M, Jamieson L, Regala RP, Weems C, Murray NR, Fields AP. A novel small-molecule inhibitor of protein kinase Ciota blocks transformed growth of non-small-cell lung cancer cells. *Cancer Res*. 2006; 66:1767–1774. [PubMed: 16452237]
- Tafforeau L, Zorbas C, Langhendries JL, Mullineux ST, Stamatopoulou V, Mullier R, Wacheul L, Lafontaine DL. The complexity of human ribosome biogenesis revealed by systematic nucleolar screening of Pre-rRNA processing factors. *Mol Cell*. 2013; 51:539–551. [PubMed: 23973377]
- Tatsumoto T, Xie X, Blumenthal R, Okamoto I, Miki T. Human ECT2 is an exchange factor for Rho GTPases, phosphorylated in G2/M phases, and involved in cytokinesis. *J Cell Biol*. 1999; 147:921–928. [PubMed: 10579713]
- Tsai RY, Pederson T. Connecting the nucleolus to the cell cycle and human disease. *FASEB journal : official publication of the Federation of American Societies for Experimental Biology*. 2014; 28:3290–3296. [PubMed: 24790035]
- Zhang ML, Lu S, Zhou L, Zheng SS. Correlation between ECT2 gene expression and methylation change of ECT2 promoter region in pancreatic cancer. *Hepatobiliary Pancreat Dis Int*. 2008; 7:533–538. [PubMed: 18842503]
- Zheng Y, de la Cruz CC, Sayles LC, Alleyne-Chin C, Vaka D, Knaak TD, Bigos M, Xu Y, Hoang CD, Shrager JB, et al. A rare population of CD24(+)ITGB4(+)Notch(hi) cells drives tumor propagation in NSCLC and requires Notch3 for self-renewal. *Cancer Cell*. 2013; 24:59–74. [PubMed: 23845442]

HIGHLIGHTS

- Ect2 is required for *Kras-Tp53* lung tumorigenesis by maintaining LADC TICs
- Ect2 binds the nucleolar transcription factor UBF1 and regulates rRNA synthesis
- Rac1 and NPM are critical effectors of Ect2-mediated rRNA synthesis
- PKC α -mediated phosphorylation regulates Ect2 binding to UBF1 and rDNA transcription

SIGNIFICANCE

The *ECT2* oncogene is overexpressed in many human cancers and is required for transformed growth. However, it is unclear how Ect2 drives transformation, and whether it is important for tumor formation in vivo. Here we demonstrate that Ect2 is required for *Kras-Trp53*-driven lung adenocarcinoma (LADC) tumor initiation in vivo, and for ex vivo growth and in vivo tumorigenicity of *Kras-Trp53* LADC tumor-initiating cells (TICs). Ect2-dependent LADC oncogenesis requires rDNA transcription activated via a PKC α -Ect2-Rac1-NPM pathway, which is blocked by the PKC α inhibitor auranofin (ANF). These data provide mechanistic insight into Ect2-mediated transformation, establish a functional link between Ect2-dependent ribosome biogenesis and LADC tumorigenesis, and reveal a therapeutic strategy for treating *KRAS*-driven LADC.

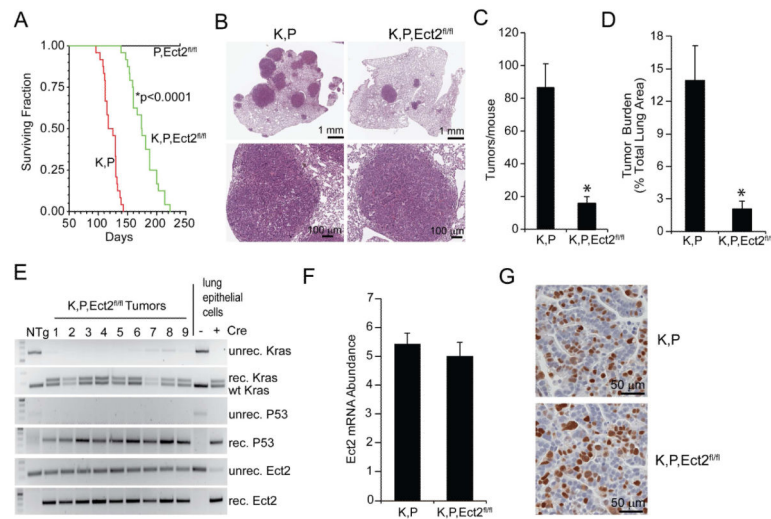


Figure 1. Ect2 is required for lung tumorigenesis in vivo

(A) Effect of genetic loss of *Ect2* on survival from *LSL-Kras^{G12D}/Trp53^{fl/fl}* (K,P) lung tumors. Kaplan-Meier analysis of K,P, K,P,*Ect2^{fl/fl}* and P,*Ect2^{fl/fl}* mice. n=25/genotype, *p<0.0001 compared to K,P mice. (B) Representative images of H&E-stained lung sections. Tumor size (C) and tumor burden (D) were assessed in K,P and K,P,*Ect2^{fl/fl}* mice 10 weeks after tumor initiation. Results represent the mean +/- SEM; n=8/genotype; *p<0.003 compared to K,P mice. (E) PCR of DNA from K,P,*Ect2^{fl/fl}* tumors for recombination of *LSL-Kras^{G12D}*, *Trp53^{fl/fl}* and *Ect2^{fl/fl}* alleles. (F) QPCR of K,P and K,P,*Ect2^{fl/fl}* lung tumors for *Ect2* mRNA. Results represent the mean +/- SEM; n=5; no significant differences were observed between K,P and K,P,*Ect2^{fl/fl}* tumors. (G) Immunohistochemical staining of K,P and K,P,*Ect2^{fl/fl}* tumors for *Ect2*. Representative images are shown. **See also Figure S1.**

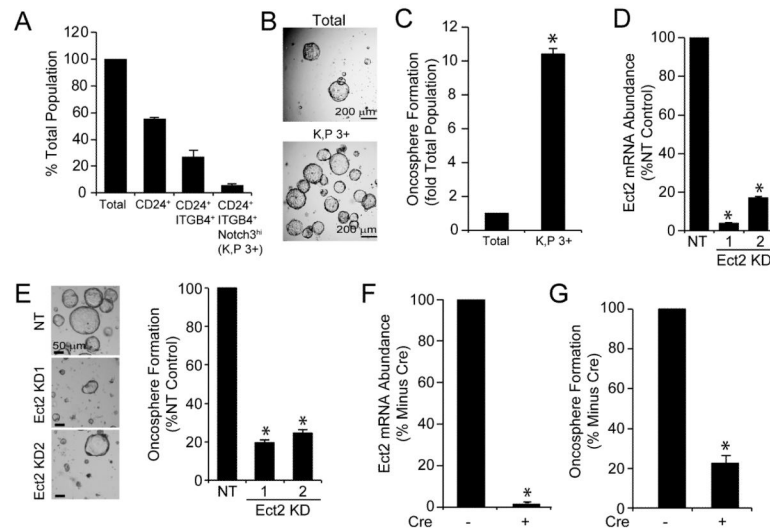


Figure 2. Ect2 is required for transformed growth of *Kras/Trp53* lung TICs ex vivo
(A) Population frequency analysis of CD24⁺/ITGB4⁺/NOTCH3^{hi} (3⁺) tumor-initiating cells isolated from K,P lung tumors. **(B)** Growth of total lung epithelial cells and K,P 3⁺ cells in Matrigel. Single cell suspensions of total epithelial and K,P 3⁺ cells were plated in Matrigel and oncospheres were quantitated after 2 weeks **(C)**. Data represent the mean \pm SEM; n=9. * $p < 1 \times 10^{-13}$ compared to total lung epithelial cells. **(D)** Effect of Ect2 KD on K,P 3⁺ cell growth. K,P 3⁺ cells transduced with mouse-specific Ect2 shRNAs or non-target control shRNA lentivirus were plated in Matrigel and assessed for oncosphere formation. Results represent the mean \pm SEM; n=10. * $p < 1 \times 10^{-6}$ compared to NT control. **(E)** Representative images of oncospheres. **(F)** and **(G)** K,P,Ect2^{fl/fl} 3⁺ cells were treated with Ad-Cre ex vivo and assessed for Ect2 mRNA **(F)** and oncosphere formation **(G)**. Results represent the mean \pm SEM; n=9. * $p < 3 \times 10^{-6}$ **(F)** and * $p < 0.0003$ **(G)** compared to no Cre. **See also Figure S2.**

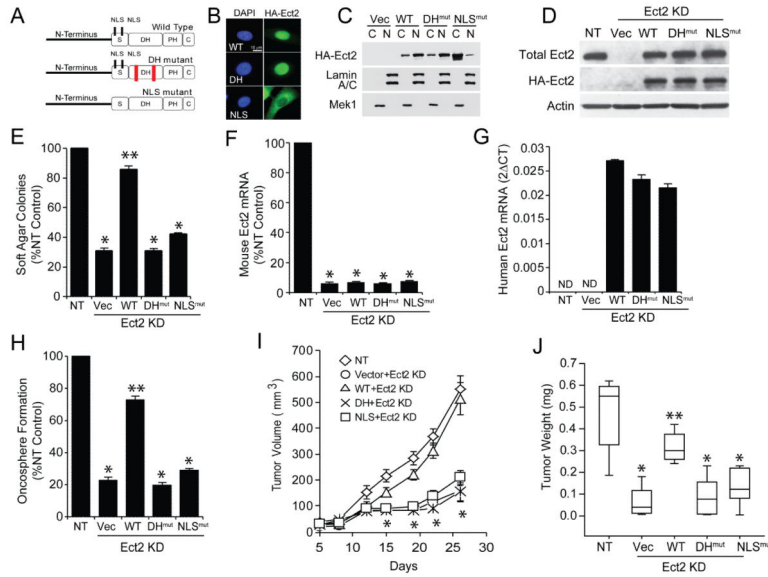


Figure 3. Ect2 is required for LADC transformed growth and tumor formation
(A) Schematic of WT, GEF-deficient (DH^{mut}) and nuclear localization sequence-deficient (NLS^{mut}) mutants. **(B)** Immunofluorescent localization of HA-tagged WT, DH^{mut} and NLS^{mut} Ect2 in transfected A549 cells using HA antibody. **(C)** A549 cells transfected with HA-tagged WT, DH^{mut} or NLS^{mut} Ect2 were fractionated into cytoplasm (C) and nucleus (N) and subjected to immunoblot analysis for HA-Ect2. Lamin A/C and MEK1 served as nuclear and cytoplasmic protein controls. **(D)** Expression of HA-Ect2 mutant alleles in Ect2 KD cells. A549 Ect2 KD cells stably transfected with HA control vector (Vec), or WT, DH^{mut} or NLS^{mut} Ect2 were subjected to immunoblot analysis for total Ect2 and HA-Ect2. Actin served as a loading control. **(E)** Effect of Ect2 KD and Ect2 alleles on transformed growth. NT cells served as positive control. Results represent the mean \pm SEM; n=5. *p < 0.0006 compared to NT cells; **p < 0.002 compared to Vec. QPCR of mouse Ect2 **(F)** and reconstitution with human Ect2 mutant cDNAs **(G)** in K,P 3+ cells. Results represent the mean \pm SEM; n=3. *p < 5×10^{-6} compared to NT. Effect of expressing WT Ect2, DH^{mut} or NLS^{mut} Ect2 on oncosphere formation in Ect2 KD K,P 3+ cells ex vivo **(H)** and tumor growth in vivo **(I and J)**. Results represent the mean \pm SEM; **(H)** n=9. *p < 3×10^{-13} compared to NT; ** p < 3×10^{-11} compared to Vec; **(I)** n=10, *p < 6×10^{-5} compared to NT; and **(J)** The tops and bottoms of the boxes indicate the 75th and 25th percentiles respectively; lines within the boxes indicate the median; lines above and below the boxes indicate the 95th and 5th percentiles respectively. n=10, *p < 0.0003 compared to NT; **p < 0.002 compared to Vec. See also Figure S3.

Author Manuscript

Author Manuscript

Author Manuscript

Author Manuscript

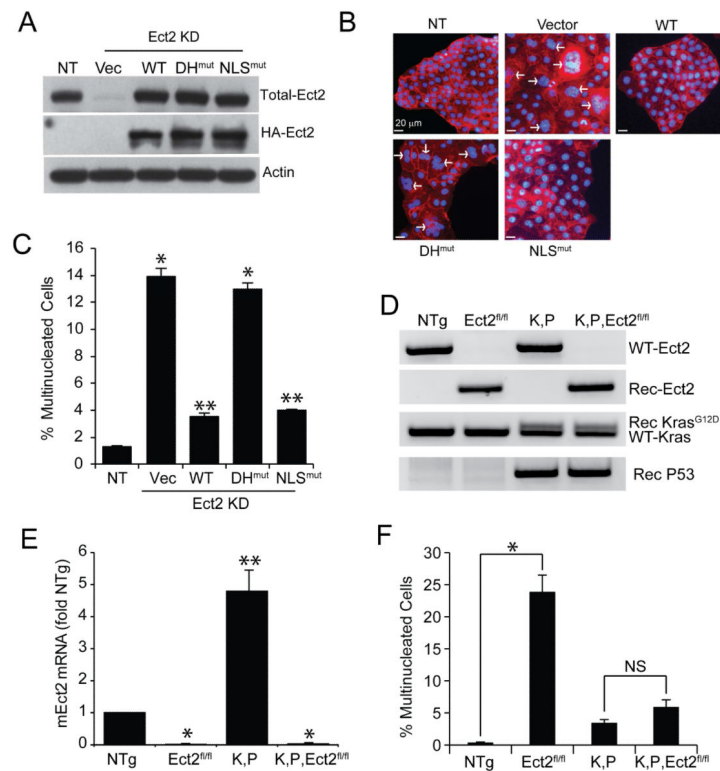


Figure 4. The role of Ect2 in transformation is distinct from its role in cytokinesis
(A) Immunoblot of Ect2KD MDCK cells transduced with HA-tagged control vector or WT, DH^{mut} or NLS^{mut} Ect2 for total Ect2, HA-Ect2 and actin. **(B)** Effect of expressing WT, NLS^{mut} Ect2, and DH^{mut} Ect2 mutants on cytokinesis (multinucleated cells) in Ect2 KD MDCK cells. Staining for phalloidin (*red*) and DAPI (*blue*). **(C)** Quantification of multinucleated cells. Results represent % multinucleated cells \pm SEM. $n > 1000$ cells from each cell type; * $p < 3 \times 10^{-21}$ compared to NT cells. ** $p < 5 \times 10^{-12}$ compared to Vec cells. **(D, E and F)** Effect of Ect2 genetic loss on cytokinesis. Primary lung epithelial cells from NTg, Ect2^{fl/fl}, K,P or K,P,Ect2^{fl/fl} mice were infected with Ad-Cre ex vivo and plated in Matrigel. Seven days post infection, cells were analyzed for recombination of *Kras*^{G12D}, *Trp53* and *Ect2* alleles by PCR **(D)**, Ect2 mRNA by QPCR **(E)**, and multinucleated cells **(F)**. Results in **(E)** represent the mean \pm SEM; $n=3$. * $p < 0.0002$ compared to NTg; ** $p < 0.001$ compared to NTg. Results in **(F)** represent the mean \pm SEM; at least 1200 cells scored for each genotype. * $p < 5 \times 10^{-8}$ compared to NTg.

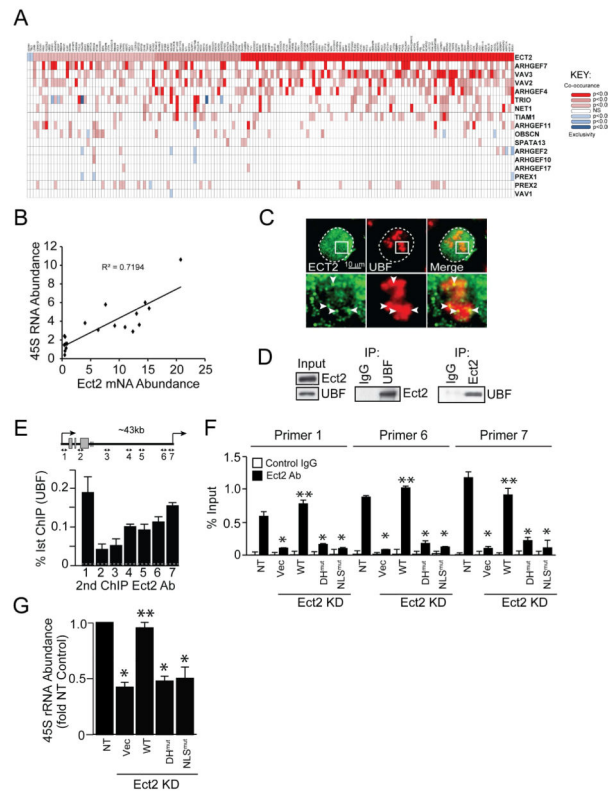


Figure 5. Ect2 localizes to the nucleolus and regulates 45S pre-rRNA synthesis
(A) Co-occurrence analysis of the TCGA LADC dataset (n=517) for expression of ribosomal processing genes and Rho family GEFs. Significant co-occurrences shown in **red** and exclusivity in **blue**. **(B)** Scatter plot showing the correlation between Ect2 mRNA and 45S rRNA in primary mutant *KRAS* LADC tumors (N=19). **(C)** Confocal immunofluorescence microscopy of A549 cells for UBF1 (**red**) and Ect2 (**green**). Merge image indicates nucleolar co-localization. Dotted line indicates nuclear boundary; Solid rectangles in upper panels indicates area shown at higher magnification in lower panels. Arrowheads indicate areas of UBF-Ect2 co-localization. **(D)** Nuclear extracts from A549 cells were immunoprecipitated for Ect2 (**right panel**) or UBF1 (**left panel**), or control IgG. Lysates (**Input**) and immunoprecipitates were immunoblotted for UBF1 and Ect2. **(E)** ChIP-reChIP analysis using sequential UBF1 and Ect2 antibody. UBF and Ect2 binding to rDNA was assessed using 7 primer sets spanning the rDNA repeat (**inset**). Results represent the mean \pm SEM; n=3. **(F)** ChIP-reChIP of NT and Ect2 KD A549 cells expressing vector, WT, DH^{mut} or NLS^{mut} Ect2 for binding to rDNA promoter regions (primers 1, 6 and 7). Results represent the mean \pm SEM; n=3. *p<0.006 compared to NT; **p<0.009 compared to Vec. **(G)** QPCR of NT and Ect2 KD A549 cells expressing the indicated Ect2 mutant for 45S pre-rRNA. Results represent the mean \pm SEM; n=3. *p<2 \times 10⁻⁶ compared to NT; **p<0.0002 compared to Vec. **See also Table S1 and Figure S4.**

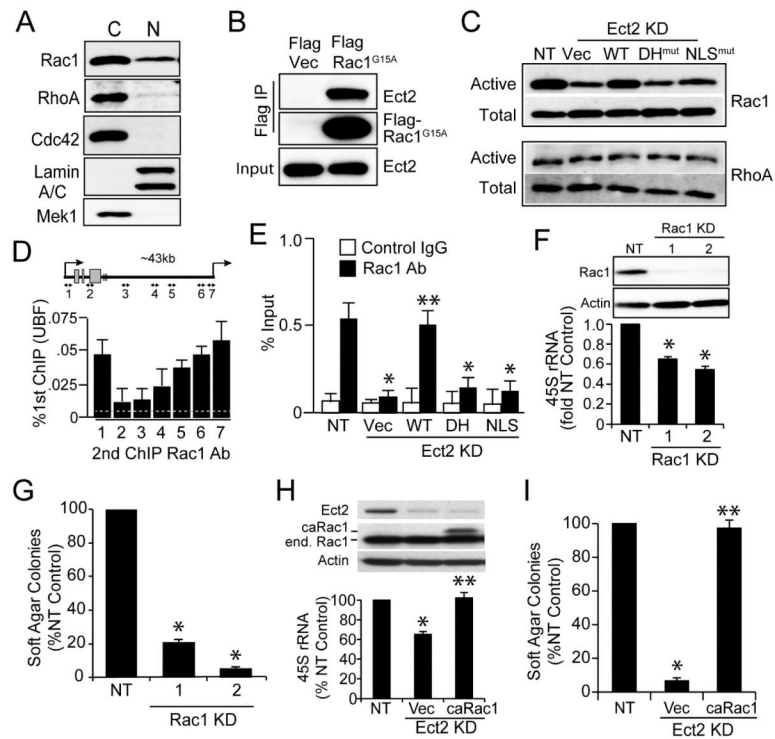


Figure 6. Rac1 mediates Ect2-dependent rRNA synthesis
(A) Immunoblot of cytoplasmic (*C*) and nuclear (*N*) A549 cell extracts for Rac1, RhoA and Cdc42. Lamin A/C and Mek1 serve as nuclear and cytoplasmic markers respectively. **(B)** Nuclear extracts expressing either empty control Vector (*Vec*) or FLAG-tagged Rac1^{G15A} were immunoprecipitated with FLAG antibody and immunoblotted for Ect2. **(C)** Nuclear extracts from NT and Ect2 KD cells expressing *Vec*, WT, DH^{mut} or NLS^{mut} Ect2 were analyzed for active, GTP-bound and total Rac1 and RhoA. **(D)** ChIP-reChIP assays using UBF1 and Rac1 antibodies for rDNA binding. Data represent the mean \pm SEM; n=3. **(E)** ChIP analysis of Rac1 binding to rDNA in NT, and Ect2 KD cells expressing Ect2 mutants. Data represent the mean \pm SEM; n=3. * $p < 0.0007$ compared to NT; ** $p < 3 \times 10^{-5}$ compared to *Vec*. **(F)** Effect of Rac1 RNAi constructs on Rac1 expression (*inset*) and 45S pre-rRNA in A549 cells. Data represent the mean \pm SEM; n=3. * $p < 0.05$. **(G)** Effect of Rac1 KD on soft agar growth. Data represent the mean \pm SEM; n=5. * $p < 4 \times 10^{-7}$ compared to NT. **(H)** Effect of constitutively active Rac1 (*caRac1*; *inset*) on 45S rDNA in Ect2 KD cells. Results represent the mean \pm SEM; n=3. * $p < 0.002$ compared to NT; ** $p < 0.004$ compared to *Vec*. **(I)** Effect of constitutively active Rac1 on soft agar growth in Ect2 KD cells. Results represent the mean \pm SEM; n=5. * $p < 8.5 \times 10^{-9}$ compared to NT cells; ** $p < 2 \times 10^{-7}$ compared to *Vec*. See also Figure S5.

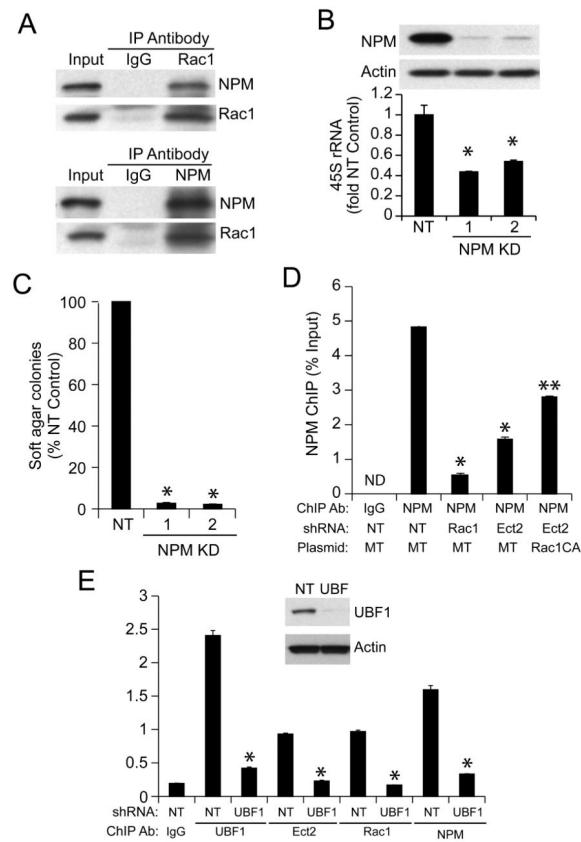


Figure 7. Nucleophosmin (NPM) binds Rac1 and mediates Ect2-, Rac1-dependent rDNA synthesis

(A) Reciprocal immunoprecipitations using NPM and Rac1 antibodies. (B) Effect of NPM RNAi constructs on NPM expression (*inset*) and 45S rRNA. Results represent the mean \pm SEM; n=3. *p<0.009 compared to NT. (C) Effect of NPM KD on soft agar growth. Data represent the mean \pm SEM; n=5. *p < 5×10^{-7} compared to NT. (D) Effect of Rac1 and Ect2 KD, and expression of caRac1 on NPM binding to rDNA (primer set 7). Results represent the mean \pm SEM; n=3. *p< 5×10^{-7} compared to NT; **p< 0.002 compared to Vec. (E) Effect of UBF1 KD (*inset*) on binding of UBF1, Ect2, Rac1 and NPM to rDNA (primer set 7). Results represent the mean \pm SEM; n=3. *p<0.001 compared to corresponding NT for each ChIP antibody. **See also Figure S6.**

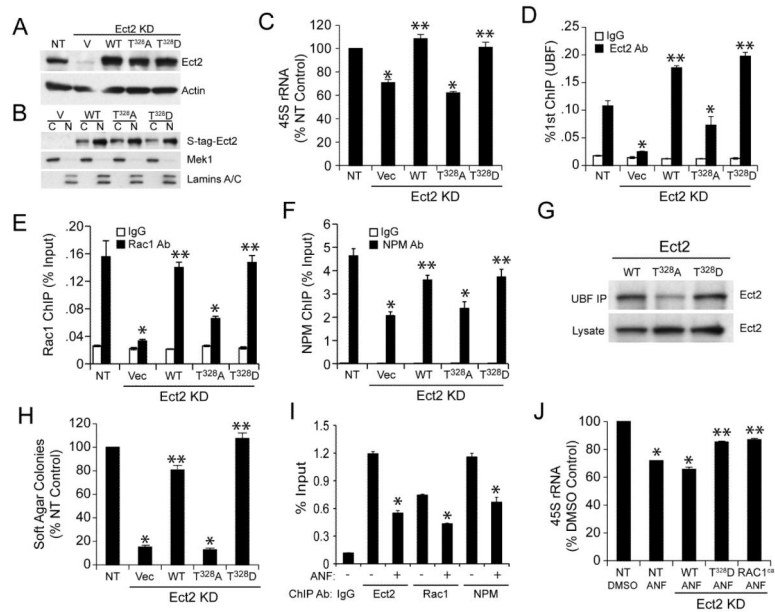


Figure 8. PKC-mediated Ect2 phosphorylation regulates Ect2-dependent rDNA binding, rRNA synthesis and transformed growth
(A) Immunoblot of Ect2 KD and expression of S-peptide tagged WT Ect2, T328A Ect2 and T328D Ect2 mutants in A549 cells. Actin served as a loading control. **(B)** Immunoblot of S-peptide tagged Ect2 alleles in cytoplasmic (**C**) and nuclear (**N**) fractions of A549 cells. MEK1 and Lamins A/C serve as markers of cytoplasm and nucleus respectively. **(C-F)** Effect of Ect2 KD and expression of WT, T328A and T328D Ect2 mutants on 45S rRNA (**C**), and on binding of Ect2 (**D**), Rac1 (**E**) and NPM (**F**) to rDNA (primer set 7). Results represent the mean \pm SEM; n=3. *p < 0.03 compared to NT; **p < 0.02 compared to Vec. **(G)** Binding of WT, T328A Ect2 and T328D Ect2 to UBF1 was assessed by immunoprecipitation/immunoblot analysis. **(H)** Effect of Ect2 KD and expression of WT, T328A Ect2 and T328D Ect2 on soft agar growth. Results represent the mean \pm SEM; n=5. *p < 3×10^{-8} compared to NT; **p < 4×10^{-7} compared to Vec. **(I)** Effect of ANF on binding of Ect2, Rac1 and NPM to rDNA (primer set 7). Results represent the mean \pm SEM; n=3. *p < 0.002 compared to corresponding DMSO control for each ChIP antibody. **(J)** Effect of ANF on 45S rRNA in NT, and Ect2 KD cells expressing WT Ect2, T328D Ect2 or caRac1. Results represent the mean \pm SEM; n=3. *p < 0.05 compared to NT treated with DMSO; **p < 0.05 compared to WT treated with ANF. **See also Figure S7.**